Quantitative mineralogical analysis of European Kupferschiefer ore

Rahfeld, A.; Kleeber, R.; Möckel, R.; Gutzmer, J.;

Originally published:

October 2017

Minerals Engineering 115(2018), 21-32

DOI: https://doi.org/10.1016/j.mineng.2017.10.007

Perma-Link to Publication Repository of HZDR:

https://www.hzdr.de/publications/Publ-25569

Quantitative mineralogical analysis of European Kupferschiefer ore

Anne Rahfeld[1*], Reinhard Kleeberg[2], Robert Möckel[1], Jens Gutzmer[1]

[1] Helmholtz Zentrum Dresden-Rossendorf, Helmholtz Institute Freiberg for Resource Technology, Chemnitzer Str.40, 09599 Freiberg, Germany

[2] Department of Mineralogy, TU Bergakademie Freiberg, Brennhausgasse 14, 09599 Freiberg, Germany

* a.rahfeld@hzdr.de +49 373139-3542

Journal: Minerals Engineering

Abstract

Kupferschiefer samples from five distinct deposits in Germany and Poland were studied with the aim to quantitatively determine their mineralogical composition using complementary approaches. Their inherently extremely fine-grained matrix, sheet silicate-dominated mineralogy, and highly variable copper sulphide content in the presence of organic components render quantitative mineralogical analysis difficult. In an attempt to develop a comprehensive yet feasible analytical routine for Kupferschiefer black shale and associated sandstone- and carbonate-hosted ores, analytical techniques were tested and adapted to suit this purpose. This study focuses on a combination of mineralogical approaches using quantitative X-ray diffraction (XRD) and image-based automatic mineral liberation analyses (MLA). Quantitative bulk-powder XRD was achieved by Rietveld refinement, based on phase identification and selection of suitable structural models. The identified minerals were verified with scanning electron microscopic measurements coupled with energy dispersive X-ray spectroscopy (EDX) and optical microscopy. Results of QXRD and MLA were compared to chemical assay data. It is concluded that MLA and QXRD deliver satisfactory results for this complex raw material, but only when

used in combination). When used independently, XRD and MLA are susceptible to significant errors related especially to sample preparation, mineral misidentification or quantification. To assure a successful quantitative mineralogical description of complex raw materials or processing products it thus is strongly recommended to verify all mineralogical information by independent analytical techniques – and to validate quantitative mineralogical information with quantitative chemical data.

Keywords: Kupferschiefer; black shale; XRD; MLA; analysis; copper sulphides; Rietveld refinement

Highlights

- Development of an analytical approach to quantify the mineralogical composition of Kupferschiefer black shales and related lithologies
- Evaluation the effects of MLA instrument settings on mineral identification
- Comparison of QXRD and MLA results
- Geochemical validation

Abbreviations

XRD: X-ray powder diffraction

QXRD: Quantitative X-ray powder diffraction

MLA: Mineral liberation analysis

EDX: Energy-dispersive X-ray spectroscopy

SEM: Scanning electron microscopy

ICP-OES: Inductively coupled plasma - optical emission spectroscopy

1. Introduction

Polymetallic sulphide ores of the Central European Kupferschiefer ore deposits (Borg et al., 2012), are currently exploited for Cu, Ag, Mo, Co, Ni, and Re in Poland with ongoing exploration in Poland and Germany. More than 37.4 Mt of Cu and 111 kt of Ag resources have been identified in Polish Kupferschiefer deposits (KGHM Polska Miedź, 2015). During recent and ongoing large-scale research into the hydrometallurgical and microbiological beneficiation of Kupferschiefer (Bioshale Project, 2007; Kutschke et al., 2015) the lack of reliable quantitative data for the mineralogical composition and microfabric for both ore as well as process samples have been identified as a major obstacle for any effort to monitor and optimize recoveries and energy efficiency (Van den Boogart et al., 2011). Similar approaches are well established for beneficiation of other Cu ores (Vorster et al., 2001; Arslan and Arslan, 2002; Kodali et al., 2011). In order to optimize resource and energy efficiency, there is an increasing need for detailed resource characterisation that goes beyond quantitative mineralogy, but includes metal deportment, mineral association, grain and particle sizes as well as liberation (Lund and Lamberg, 2014). However, a satisfactory quantification of mineralogical and textural parameters has not been achieved for Kupferschiefer ores, mainly due to the inherently complex composition of the material. This is despite the fact that Kupferschiefer ores have been the subject of many mineralogical studies. Previous studies have typically focused on particular parameters, such as sulphide mineralogy (Kucha, 1982; 1993; Large et al., 1995; Kucha and Pryblowicz, 1999; Piestrzynski and Pieczonka, 2012), sheet silicate mineralogy (Vaughan et al., 1989; Bechtel et al., 1999; Bechtel et al., 2000) or the presence and abundance of organic

carbon (Püttmann et al., 1991). Despite this abundance of detailed investigations there is an obvious lack of a holistic view of the mineralogy of Kupferschiefer-type ores.

Kupferschiefer *sensu stricto* refers to a carbonaceous black shale unit with a thickness of a few centimetres up to a meter that was deposited in response to rapid marine transgression into an intracontinental sedimentary basin during the Permian age (Wedepohl, 1964; Vaughan et al., 1989; Paul, 2006). Stratabound sulphide mineralization is widespread along the southern margin of the sedimentary basin (Borg et al., 2012). The Kupferschiefer *s.s.* is bounded by a lower sandstone and an upper carbonate unit, respectively. Sulphide mineralization occurs in all three lithotypes that together comprise the geological resource of the Kupferschiefer (Borg et al., 2012). Host rock, ore mineralogy, and grade vary greatly not only between the different lithotypes, but also along local and regional trends within the different lithotypes. Ore within the Mansfeld district, for example, is essentially confined to the Kupferschiefer s.s., in comparison to the Sieroszowice ore in Poland, where a very significant proportion is contained in sandstone and carbonate lithotypes (Wedepohl, 1964; Paul, 2006; Borg et al., 2012). The origin of the polymetallic mineralization is not well constrained, but is likely related to multi-stage dia- to epigenetic hydrothermal fluid flow events (Michalik and Sawlowicz, 2001; Borg et al., 2012).

The ore mineralogy of the Kupferschiefer s.s. is exceptionally complex. Styles of mineralization range from finest dissemination (Fig. 1) and coarser replacement and impregnation to vein- and breccia-hosted sulphide mineralization. More than 80 ore minerals have been described in the Kupferschiefer ore (Piestrzynski and Pieczonka, 2012), with Cu contained mostly in chalcocite-group minerals, bornite, and chalcopyrite. Of importance as ore minerals are further sphalerite, galena, enargite, cobaltite, and tennantite (Vaughan et al., 1989; Matlakowska et al., 2012).

Noble metals (Au, Ag and PGMs) occur in sulphides and as discrete minerals (Vaughan et al., 1989; Piestrzynski and Sawlowicz, 1999; Piestrzynski and Pieczonka, 2012).

A further characteristic of Kupferschiefer s.s. is the very fine-grained matrix composed of sheet silicates, namely illite, kaolinite, and chlorite. These sheet silicates, commonly clay sized (<2µm), can account for more than 50 wt% of the Kupferschiefer s.s. The sheet silicates are very finely intergrown with variable amounts of carbonate minerals, namely calcite, dolomite, and ankerite (Wedepohl, 1964; Bechtel et al., 2000; Matlakowska et al., 2012). Finally, Kupferschiefer s.s. contains up to 30 wt % organic matter (C_{org}), with an average of about 5 wt% (Speczik et al., 1995). The organic matter has been characterized as kerogen type II, primarily of marine origin, with the addition of minor amounts of type III (Sun and Püttmann, 2004). This organic carbon forms thin bedding parallel lenses and is finely disseminated between sheet silicates and carbonate minerals (Fig. 1).

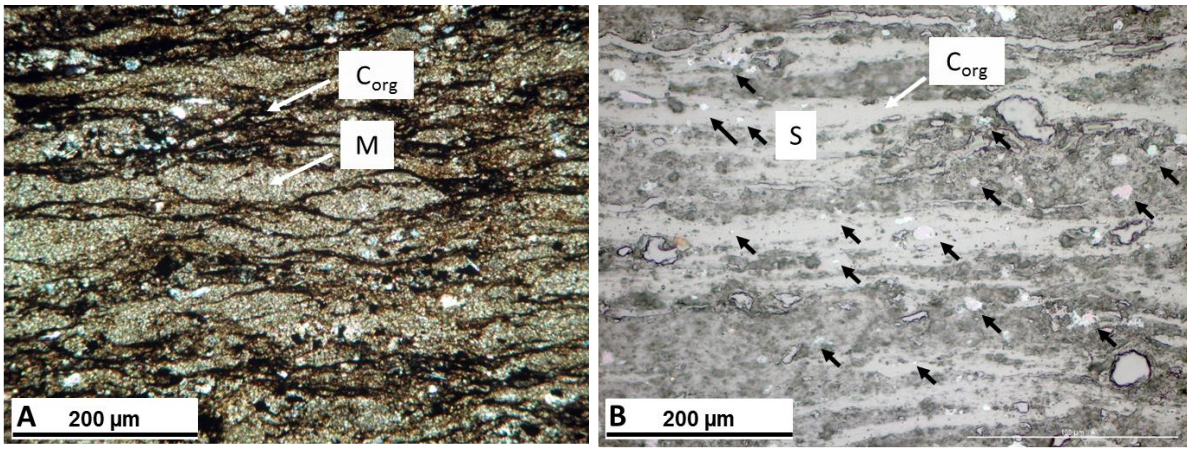

Figure 1: A - Photomicrograph of Kupferschiefer s.s. sample P-KS-02 (left) illustrating the fine-grained texture of the sheet silicate and carbonate-rich matrix (M) with irregular lenses and layers of organic matter (C_{org}). B - Photomicrograph in reflected light of sample P-KS-03 showing dissemination of copper sulphides (S, black arrows)

Complex mineralogy, fine-grained texture, disorder and structural variability of the clay minerals, and amorphous nature of the organic component, all pose significant challenges for the comprehensive and quantitative mineralogical characterization of Kupferschiefer ore.
In this investigation, we employ a combination of quantitative X-ray diffraction (QXRD) and SEM-based image analysis (MLA) (Fig. 2) to investigate pitfalls and find possible solutions for the quantitative mineralogical characterization of the Kupferschiefer s.s. The analytical methods applied are largely complementary. Minerals are identified by the attributes of their crystal structure by X-ray powder diffractometry, whilst SEM-based image analysis relies on compositional contrast in mineral chemistry. Results of quantitative X-ray powder diffractometry (QXRD) by multiphase Rietveld refinement (Rietveld, 1967; Hill and Howard, 1987) can be highly accurate and allow the quantification of abundances of minerals present down to 0.5 wt% in representative powder samples (König and Spicer, 2007; Parian et al., 2015). However, an increase of the number and crystallographic complexity of the contained minerals (Omotoso et al., 2006; Parian et al., 2015), and the presence of amorphous materials render reliable quantification by QXRD increasingly difficult.

SEM-based image analyses (Gu, 2003), in contrast, allows the reliable identification even of trace minerals (i.e. has a lower detection limit) and the reliable quantification of mineral abundances well below 1 wt% (Fig. 2). Furthermore, MLA provides numerical values for microfabric attributes such as grain size and shape, mineral associations and mineral liberation. However, SEM-based image analysis does not permit differentiation of polymorphs or minerals that have a very similar mineral chemistry (e.g., chalcocite and digenite; Weissflog et al., 2011). An even more profound limitation of SEM-based image analysis concerns the fact that analysis is

always limited to a 2D surface, rather than a 3D volume, as well as the limit of lateral resolution that can be attained during EDX analysis using an electron beam. As a result of the extremely fine grain sizes, encountered in the Kupferschiefer s.s, EDX spot analyses report compositional information not only from the mineral grain in question, but also from surrounding grains. Such mixed spectra are difficult to assign to a single mineral (Kern et al., 2017).

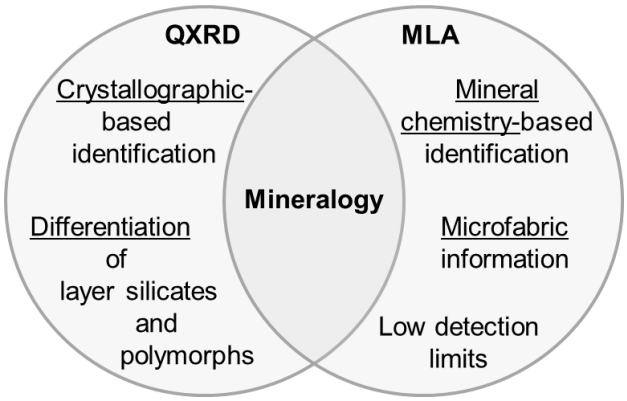

Figure 2: Schema of method-specific characteristics and advantages

From the above it is evident that both QXRD and MLA are pushed to their technical and physical limits in the analysis of Kupferschiefer-type ores. This study attempts to identify and minimize common errors and assess the validity of the results by using geochemical data in support. The accuracy of the analyses cannot be evaluated directly by using either a reference standard or a synthetic mixture, since no Kupferschiefer standard presently exists and the preparation of a synthetic mixture will not represent the complexities inherent to the Kupferschiefer ore.

2. Materials and methods

The Kupferschiefer ore samples analysed in this study originate from five different localities (Tab. 1). These include mineralised Kupferschiefer s.s. from the underground Wettelrode Fortschritt shaft and a bulk sample collected from a Kupferschiefer dump in the Mansfeld region

of Germany. Additional mineralised Kupferschiefer s.s., mineralised sandstone, and mineralised carbonate rock samples were collected from the active Rudna and Polkovice-Sierocowice mines in Poland to investigate potential obstacles to the characterization of the different lithotypes. The Kupferschiefer s.s. samples were selected specifically to represent the high degree of variability in clay, carbonate copper sulphide, and organic carbon content (1-14 wt%) that is commonly encountered in Kupferschiefer deposits (Wedepohl, 1964; Vaughan et al., 1989; Paul, 2006). An industrial Cu-rich sulphide concentrate (L-KS-Con) supplied by KGHM was included in the study, representing a flotation concentrate obtained from a mixture of ore lithotypes and locations.

Table 1: List of sampling locations and lithological types (an industrial sulphide flotation concentrate originating from a mixture of Kupferschiefer black shale, sandstone, and carbonate)*

	Wettelrode	**Mansfeld**	**Polkowice**	**Rudna**	**Lubin**
Kupferschiefer s.s.	W-KS	M-KS	P-KS-2 P-KS-3	R-KS	
Sandstone			P-Sa-10	R-Sa	
Carbonate				R-Ca	
Concentrate					L-KS-Con*

At least 3kg of each sample were collected and crushed to < 15mm. To minimize damage to crystal structures and related amorphisation, a representative fraction of 200 g of the material was split off for manual grinding to 100 µm and subsequent analysis of the sheet silicates. The remaining material was milled down to 90 µm with a ball mill, and then split further for chemical and mineralogical analysis. Material intended for XRD analyses was milled with a McCrone mill to minimize micro-absorption effects caused by large crystallite sizes.

2.1. Sheet silicate separation

Manually ground material of all samples (excluding the concentrate sample L-KS-Con), underwent additional pre-treatment steps to remove carbonate minerals and organic matter in order to optimize the sheet silicate recovery of the Atterberg method for grain size separation and to obtain clean, unobscured XRD peaks of the clay minerals (Moore and Reynolds, 1989). The sheet silicates were separated and analysed without any pre-treatment, to ensure that no alteration occurred within the minerals as a result of chemical treatment. Removal of organic matter was completed with hydrogen peroxide (Jackson, 1979) at a temperature of 40°C. Carbonate minerals were removed by dissolution in 0.5 N HCl following Jackson (1979). The supernatant was rinsed with deionized water until no chloride could be detected by the addition of $AgNO_3$. A suspension of 10 g of the remaining material with 100 ml deionized water and 10 ml $Na_2P_2O_7$ was prepared overnight to aid the dispersion of the sheet silicate. A complete separation of the fraction smaller 2 µm required six to seven runs with the Atterberg method.

2.2. XRD

XRD measurements were done with a PANalytical Empyrean diffractometer at the Helmholtz Institute Freiberg for Resource Technology (HIF), using a common Xe-proportional counter detector in combination with a graphite monochromator to supress Kβ and fluorescence radiation. Co radiation at 35 kV and 35 mA was applied. A step size of 0.015° 2Θ in the range of 5° to 80° 2Θ and a step time of 20 sec/step were set. In addition, samples P-KS-03 and L-KS-Con were measured with 40 sec/step to achieve a better peak to noise ratio and clearer peak identification. The software package HighScore 3.0 supplied by PANalytical was used for mineral identification and for Rietveld refinement the BGMN/Profex v3.8.0 bundle was used (Doebelin and Kleeberg, 2015).

Corundum (20 wt%) was added as internal standard to the sample material in order to determine amorphous (i.e. organic) contents. Structure models for the Rietveld analysis were selected basing on database matches, optical microscopy, XRD of large (80-100 µm) hand-picked grains and EDX measurements to examine their chemical composition. To minimize textural/preferred orientation effects, samples were side-packed (side loading technique, Brown and Brindley 1980). Triplicates were prepared and measured to determine the standard deviation. Three texture-free samples were additionally prepared by spray-drying (Hillier, 1999) for reference purposes.

For clay mineral identification of oriented samples, a Seifert/Freiberger Präzisionsmechanik HZG4 device was used, equipped with Cu-Kα radiation (40kV, 40mA), diffracted beam graphite monochromator, and scintillation detector. Data was collected between 2-34°2Θ with a step width of 0.03°2Θ at 8s/step. The Sybilla© software developed by Chevron™ (Zeelmaekers et al., 2007) was used to simulate potential sheet silicate compositions. The measurements were completed at the Department of Mineralogy of the Technische Universität Bergakademie Freiberg.

2.3. MLA

Quantitative mineralogical analysis using MLA was carried out on polished and carbon-coated grain mounts. The grain mounts were made of a mixture of 3g milled (P_{100} <90 µm) sample material with 2g epoxy resign at the sample preparation laboratory of the HIF. The ratio of sample material and epoxy was chosen as to minimize sedimentation effects during preparation.

The MLA system used comprises a scanning electron microscope FEI Quanta 650F equipped with two Bruker Quantax X-Flash 5030 energy-dispersive X-ray spectrometers and the MLA software Suite 3.1.4 for automated data acquisition and evaluation. Grain-based X-ray mapping (GXMAP; Gu, 2003) was chosen as measurement mode, because of the small differences in grey scale between carbonate and sheet silicates as well as between the different copper sulphides. GXMAP-collected EDX spectra at each point within a grid of 1.5 µm for all mineral grains that fell within a pre-set BSE grey-scale range. The MLA measurements were carried out at the Geometallurgy Laboratory at the Technische Universität Bergakademie Freiberg (TUBAF).

A selection of five samples was studied in greater detail (R-KS, R-Sa, R-Ca, P-KS-02, P-KS-03, L-KS-Con), including measurements of three different parts of each grain mount, each amounting to 150.000-250.000 particles, to determine intra-sample variability related to sample heterogeneity or sample preparation. An average and standard deviation was calculated from this data.

Series of analyses were carried out at acceleration voltages of 15 and 25 kV within the same areas of the grain mounts to ascertain optimal measurement parameters – primarily to assess the amount of mixed spectra which negatively influence the data evaluation. The results showed distinct and systematic differences. These differences can be attributed to the increased excitation volume of the electron beam in the sample at 25 kV – as compared to 15 kV. The larger excitation volume, of ~5-6 µm in carbonates and sheet silicates at 25 kV compared to ~2 µm at 15 kV, results in a rapid increase in the number of mixed spectra. This leads to a strong underestimation of silicate mineral abundances, caused by high amounts of mixed spectra generated within the fine-grained, sheet silicate-dominated matrix, and respective overestimation of copper mineral abundances. Results obtained at 25 kV were thus

disregarded, despite the fact that analyses at higher acceleration voltages had the benefit of the more accurate identification of the copper mineral species (e.g. distinction of chalcopyrite from bronite).

Mineral identification and quantification was done based primarily on EDX analysis but also back-scattered electron image information in combination with the mineralogical information collected by XRD. The mineral list used in the automated mineralogical analysis consists of 50 different minerals. Individual spectra were collected for every mineral found within the sample material. For clarity, only data aggregated into logical mineral groups are presented in this contribution. Minerals were grouped together as carbonate minerals (including calcite, dolomite, ankerite), sheet silicates (including white mica, kaolinite, Fe-rich sheet silicates), accessory and gangue minerals (including gypsum, barite, celestine, albite, orthoclase/microcline, apatite, rutile), copper sulphides (bornite, chalcopyrite, chalcocite, covellite), and other sulphides (including pyrite, marcasite, sphalerite, galena). Unidentified spectra, often obtained from mineral mixtures (i.e. mixed spectra), were classified as unknowns. Occasional mismatches in the identification of EDX spectra required the application of advanced classification that manually defined size and position of necessary peaks (Fe in case of bornite and ankerite). All mineralogical data reported in this study was normalized to 100 wt%, excluding unknowns and organic compounds. Organic compounds could not be identified because conventional epoxy resin was used in samples preparation. This method does not allow for recognition of solid organic matter. The use of iodized epoxy resin (Rahfeld and Gutzmer, 2017), is recommended for future studies to generate quantitative mineralogical data including the abundance of solid organic carbon.

2.4. Chemical assay data

Quantitative chemical assay data for the nine studied samples was acquired by ICP-OES analyses at the Department of Mineralogy of the TU Bergakademie Freiberg; a peroxide digestion method using Na_2O_2 was applied (Tab. 2; Rahfeld et al., submitted 2017; Operating instruction FXSOP-0083-01, FluXana GmbH & Co.). Standard deviation is given for double measurements. Concentration data obtained for Si, Al, Ca, and Cu were used to assess the accuracy of the XRD and MLA results. A previous study regarding the reliability of geochemical analyses of Kupferschiefer indicated a common underestimation of Cu by 5% and Al by 12% relative to instrumental neutron activation analysis (Rahfeld et al., submitted 2017). Ca had an uncertainty of 3 to 7 % but was within the INAA measurement uncertainty. No reliable INAA-Si data is available, but comparison with reference materials suggests an underestimation of about 3 to 8%. The organic content determined separately by elemental C/N/S analysis was considered in the calculation of the inorganic mineralogical data.

Table 2: ICP-OES data used in the data validation (values in wt%)

Samples	Si	Al	Ca	Cu
P-KS-2	15.27 ± 0.17	5.66 ± 0.37	8.88	6.67 ± 0.06
P-KS-3	14.29	5.71	0.89	28.00
P-Sa	-	1.80	2.12	17.00
R-KS	11.25 ± 0.05	5.34 ± 0.03	11.85 ± 0.15	3.97 ± 0.02
R-Sa	-	2.56	2.64	2.89
R-Ca	6.71	2.89	17.80	2.60
M-KS	15.89	5.18	8.61	0.64
W-KS	15.78 ± 0.59	6.33 ± 0.12	2.72 ± 0.02	2.67 ± 0.09
L-KS	8.70	3.91	3.94	15.00

3. Results

A combination of powder XRD, MLA, optical microscopy and single grain XRD analysis enabled a successful identification and assessment of the mineralogical composition of the Kupferschiefer samples. Overall, 40 minerals were identified (Tab. 3).

Table 3: List of identified and Rietveld refined minerals considered for Rietveld refinement – and the grouping applied to the data for comparability (sorted based on relative abundance)

Grouping	Identified minerals			
Quartz	Quartz	SiO_2		
Sheet silicates	White mica (2M1+1Mt)	$KAl_2(Si_3Al)O_{10}(OH,F)_2$		
	Chlorite	$(Mg,Fe)_5Al(Si_3Al)O_{10}(OH)_8$		
	Kaolinite	$Al_2Si_2O_5(OH)_4$	Dickite	$Al_2Si_2O_5(OH)_4$
Carbonates	Dolomite[1]	$CaMg(CO_3)_2$; $Ca(Ca_{0.08}Mg_{0.92})(CO_3)_2$)		
	Calcite	$CaCO_3$	Ankerite	$Ca(FeMg)(CO_3)_2$
Copper minerals	Chalcocite	Cu_2S	Bornite	Cu_5FeS_4
	Djurleite	$Cu_{31}S_{16}$	Roxbyite	$Cu_{1.78}S$
	Digenite	Cu_9S_5	Covellite	CuS
	Chalcopyrite	$CuFeS_2$	Atacamite	$Cu_2Cl(OH)_3$
	Azurite	$Cu_3(CO_3)_2(OH)_2$	Malachite	$Cu_2CO_3(OH)_2$
	Tennantite	$Cu_{12}As_4S_{13}$		
Other sulphides	Pyrite	FeS_2	Galena	PbS
	Sphalerite	ZnS	Marcasite	FeS_2
Accessories	Albite	$NaAlSi_3O_8$	Microcline	$KAlSi_3O_8$
	Orthoclase	$KAlSi_3O_8$	Barite	$BaSO_4$
	Anhydrite	$CaSO_4$	Gypsum	$CaSO_4*2(H_2O)$
	Anglesite	$PbSO_4$	Apatite	$Ca_5(PO_4)_3OH/Cl$
	Celestine	$SrSO_4$	Rutile/Anatase	TiO_2
	Enargite	Cu_3AsS_4	(Ni-) Cobaltite	(Co,Ni)AsS
	Titanite	$CaTiSiO_5$	Stromeyerite	AgCuS
	Zircon	$ZrSiO_4$	Cerussite[2]	$PbCO_3$

1 Dolomite as well as Ca-disordered dolomite 2 Secondary mineral in processing products (L-KS-Con)

Averaged results of QXRD and MLA measurements are presented in direct comparison and do not include amorphous contents and classified unknowns, which also contain organic matter (Figure 3; Tab. 4). Overall, each lithological type is characterized by a distinct mineral assemblage. All Kupferschiefer shale samples contain a similar concentration and ratio of sheet silicates to carbonate minerals to quartz. Highly variable is the copper mineral content. Sample

W-KS stands out with a much elevated sheet silicate and reduced carbonate mineral content. Expectedly, quartz concentrations above 50 wt% were found in sandstones and about 60 wt% carbonate minerals in the carbonate ore. The distribution of the carbonate minerals varies. Dolomite is the predominant mineral in the carbonate ore, while calcite is more common in sandstone ore. Dolomite and calcite content are variable in the shale ore. Galena and pyrite are enriched in samples from Rudna and L-KS-Con.

Comparison shows consistently higher sheet silicate and copper sulphide contents detected by MLA relative to QXRD and reduced carbonate contents. Data acquired by QXRD, also has a higher content of minerals classified as accessories, especially the case in L-KS-Con. This is primarily caused by higher concentrations of barite, celestine, gypsum, anhydrite, and partially feldspars.

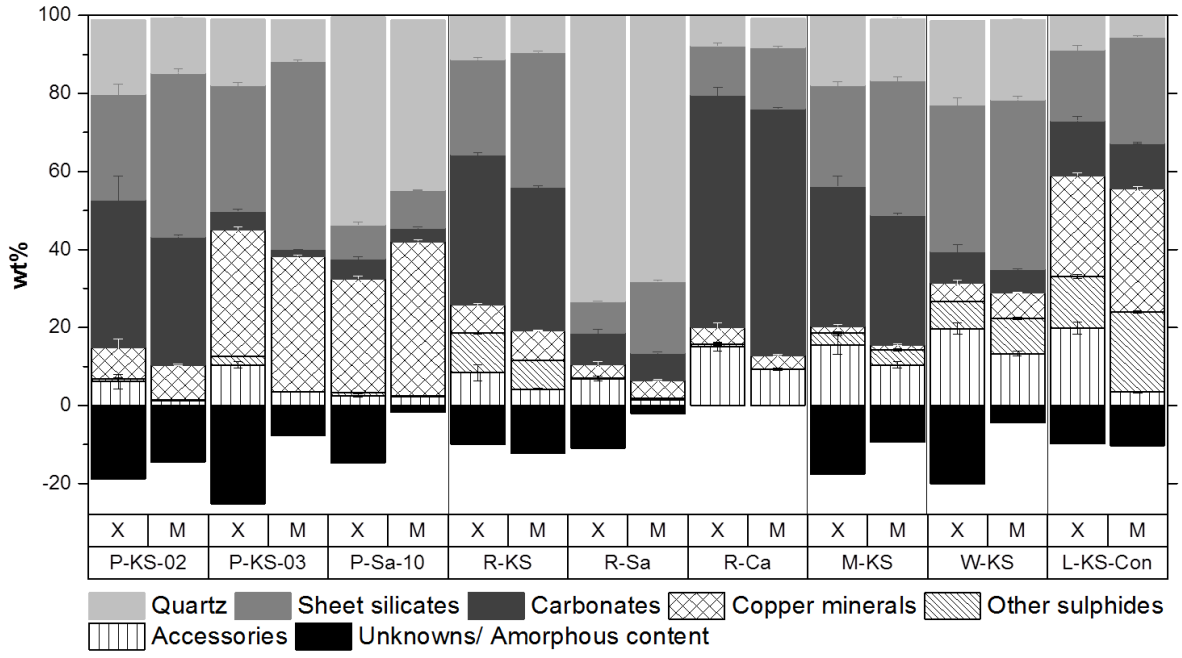

Figure 3: Illustration of quantitative mineralogical results of QXRD (X) and MLA (M). Results normalized to 100 wt% excluding unknowns and amorphous contents.

Table 4: List of quantitative mineralogical results in wt %, including STD as determined by triple measurements

XRD	Quartz	Sheet silicates	Carbonate minerals	Copper minerals	Other sulphides	Accessories	Amorphous content
P-KS-2	19.2 ± 0.1	27.1 ± 2.6	37.8 ± 3.8	8.0 ± 2.2	< 1 ± 0.2	6.1 ± 1.9	18.9
P-KS-3	16.8 ± 0.1	32.4 ± 0.7	4.8 ± 0.6	32.4 ± 0.8	< 1 ± 0.1	10.4 ± 0.9	25.2
P-Sa	53.3 ± 0.3	8.6 ± 0.8	5.2 ± 0.5	29.2 ± 0.8	< 1 ± 0.1	2.5 ± 0.4	14.7
R-KS	11.3 ± 0.2	24.5 ± 1.0	38.5 ± 1.8	7.3 ± 0.8	10.1 ± 0.3	8.4 ± 2.1	9.9
R-Sa	74.0 ± 0.8	8.0 ± 0.2	8.1 ± 1.0	3.4 ± 0.8	< 1 ± 0.05	6.9 ± 0.7	10.9
R-Ca	8.1 ± 0.2	12.5 ± 0.9	59.5 ± 1.8	4.4 ± 1.0	< 1 ± 0.3	15.1 ± 1.1	
M-KS	17.9 ± 0.1	25.9 ± 0.8	35.9 ± 2.7	1.7 ± 0.4	3.1 ± 0.3	15.5 ± 2.4	17.6
W-KS	21.6 ± 0.1	37.5 ± 1.8	8.1 ± 1.8	4.8 ± 0.7	6.9 ± 0.1	19.7 ± 1.5	20.1
L-KS	7.9 ± 0.1	17.2 ± 0.6	13.2 ± 1.1	24.8 ± 0.8	13.3 ± 0.6	19.8 ± 1.5	9.8

MLA	Quartz	Sheet silicates	Carbonate minerals	Copper minerals	Other sulphides	Accessories	Unknowns
P-KS-2	14.0 ± 0.2	42.0 ± 1.0	32.9 ± 0.4	9.0 ± 0.2	< 0.1	1.3 ± 0.2	14.5
P-KS-3	10.6 ± 0.1	48.2 ± 0.3	1.8 ± 0.1	34.7 ± 0.4	< 0.1 ± 0.1	3.5 ± 0.1	7.6
P-Sa	42.6 ± 0.2	9.7 ± 0.1	3.5 ± 0.3	39.6 ± 0.4	< 0.1 ± 0	2.3 ± 0.1	1.7
R-KS	9.9 ± 0.1	34.6 ± 0.3	36.9 ± 0.4	7.6 ± 0.1	7.4 ± 0.1	4.2 ± 0.2	12.2
R-Sa	68.2 ± 0.3	18.3 ± 0.3	7.0 ± 0.3	4.6 ± 0.2	0.3 ± 0.1	1.5 ± 0.1	2.1
R-Ca	7.4 ± 0	15.8 ± 0.2	63.1 ± 0.4	3.6 ± 0.2	< 0.1	9.2 ± 0.3	10.7
M-KS	15.8 ± 0.5	34.5 ± 0.9	33.2 ± 0.6	1.3 ± 0.2	3.9 ± 0.4	10.4 ± 0.8	9.4
W-KS	19.0 ± 0.2	42.1 ± 0.8	4.9 ± 0.2	5.4 ± 0.1	8.0 ± 0.3	13.3 ± 0.6	4.5
L-KS	5.7 ± 0.1	27.1 ± 0.3	11.7 ± 0.2	31.7 ± 0.6	20.5 ± 0.3	3.4 ± 0.3	10.3

3.1 Sheet silicate mineralogy

Quantification of sheet silicates, that are found in abundance within Kupferschiefer-type ores and dominate the black shale composition, is complicated by disorder related to defects by rotations or translations of layers within the stacking (Bish, 1993; Hillier, 2000; Ufer et al., 2012). Using XRD analyses of the separated clay size fraction in samples from Mansfeld and Polkowice-Sieroszowice five types of sheet silicates were identified. Chlorite was present in most samples, but played only a minor role with an overall concentration of 0.5 to 2 wt% within the whole rock samples. A more detailed study of the chlorite was not attempted due to the overabundance of white micas obstructing any calculation. Kaolinite group minerals occur in the samples and were identified based on peak positions and thermal treatment as kaolinite and dickite (Fig. 4; Hill,

1955). It is noticeable that kaolinite and dickite are significantly enriched relative to white mica within the sandstone samples (Fig. 5). However, white mica comprises the bulk of sheet silicates present in all samples. This white mica fraction may comprise of illite and/or muscovite. A precise differentiation between muscovite and illite can only be made based on the measured K-deficiency (Bailey, 1984), which was not attempted in this project. Swelling induced by ethylene glycol was used to identify the proportion of interstratified smectitic layers (Fig. 3). According to the results, the estimated content of mica-smectite interstratifications amounts to less than 10% of the overall white mica found in the samples (Fig. 4, 5). In addition, $2M_1$ and 1M polytypes and rotationally disordered $1M_d$ varieties were recognized within random powder (Fig. 5) prepared by spray-drying (Hillier, 1999).

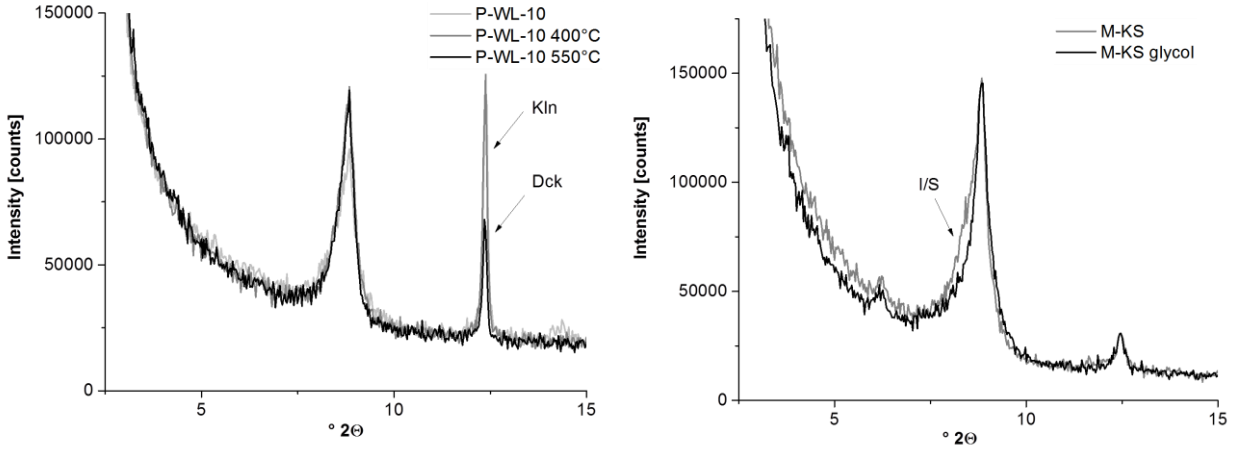

Figure 4: XRD patterns of oriented aggregates after heat treatment (left), used to identify proportions of kaolinite (Kln) and dickite (Dck), and glycolation with ethylene glycol (right), used to identify fractions of illite-smectites (I/S)

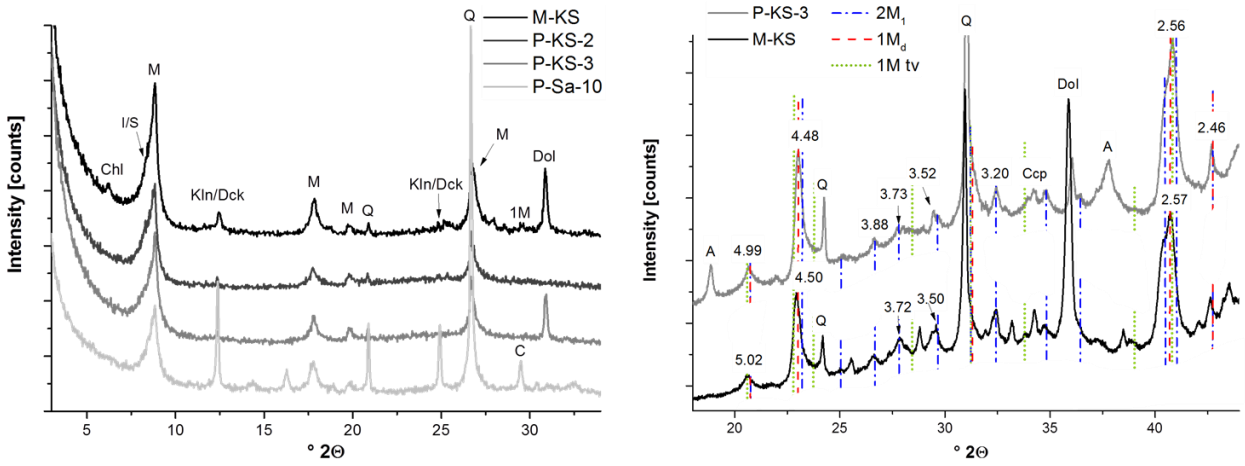

Figure 5: Selection of oriented XRD measurements (left) illustrating the variety of clay minerals associated with Kupferschiefer ores and patterns of randomly oriented samples (right) prepared by spray-drying showing white mica polytpes based on Drits et al., 1993 (d-values in Å, Chl: chlorite, I/S: mica-smectite, M: white mica, Q: quartz, Kln: kaolinite, Dck: dickite, Dol: dolomite, A: atacamite, Ccp: chalcopyrite)

The presence and combination of various sheet silicates and polytypes have restricted the originally proposed goal of building a suited specialized structural model for white mica in Kupferschiefer. A structural study of the white micas could not be completed, even within an oriented sample measurement of the pre-treated clay size fraction, primarily due to the overwhelming presence of mica polytypes $2M_1$ and $1M_d$ obscuring most distinguishing attributes. An attempt was made to use a model for rotationally disordered illite structure including interstratified smectitic layers (Ufer et al., 2012), but resulted in day-long calculation times and no significant change in the quantified mineralogy. Based on these results and trials with various structural models, Rietveld refinement was concluded with models of ordered kaolinite (Bish, 1993), dickite (Bailey, 1963) , chlorite (Steinfink, 1958; Bergmann and Kleeberg, 1998), muscovite $2M_1$ (Birle and Tettenhorst, 1968) and illite 1Mt (Tsipursky and Drits, 1984).

3.2 Results of QXRD

Extensive peak overlaps are encountered in analyses of Kupferschiefer ores that contain more than 25 minerals and render routine quantitative phase analysis based on the integral peak intensities precarious. Furthermore, potential misidentification of minerals with very similar or identic crystal structure is possible, especially in the presence of overlapping peaks, and differences in the absorption of X-rays between silicates and sulphides have to be considered (Bish, 1988; Taylor and Matulis, 1991). These concerns were addressed by the application of diverse analytical techniques and cross-verification. QXRD yielded comprehensive data on the abundance of all major mineralogical constituents and their structures. In the case of dolomite, more than one crystal structure had to be used in the refinement process. Initial Rietveld refinements assumed an overabundance of ankerite (concluded from enhanced lattice parameters versus pure dolomite endmember) that was not supported by EDX measurements. EDX data proved the absence of iron from most carbonate mineral grains. The misidentification was caused by an excess of Ca in Ca-disordered dolomite that shares peak positions with ankerite. A structural file based on Drits et al. (2005): ICSD-152201 was added to the calculation and the refined fit of ankerite was restricted. Carbonate minerals were quantified with a high average standard deviation of about 8 % due to the difficulties encountered in the simultaneous refinement of two very similar dolomite structures. The highest standard deviation between triple measurements was observed for the group of copper sulphides, in particular in samples containing less than 5 wt% copper sulphide minerals. This is partially owed to detailed information gained by Rietveld analysis and its excellent ability to distinguish the structurally variable copper sulphides djurleite, roxbyite, and digenite from chalcocite. Most of these copper minerals range within 1 and 2 wt%. Such low concentrations cannot be determined with a high accuracy using Rietveld refinement in a complex material such as the Kupferschiefer, due to

extensive peak overlaps. In addition, it should be noted that mineralogical changes can occur in the finely ground material, specifically within the copper sulphides, when using sample material that has not been freshly prepared. A common transition of djurleite into roxbyite could be observed in aging milled samples (Fig. 6). It is speculated, that a sulphur-rich atmosphere develops within the closed vials of the sample powders over time and causes that change.

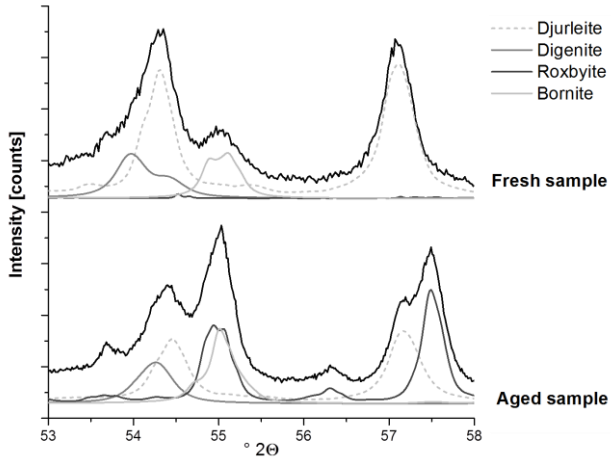

Figure 6: Portion of diffractogram illustrating the change in the copper sulphide mineralogy of sample P-KS-3 within a fresh (top) and an aged, 6-month old sample (bottom)

A major factor in the evaluation of the accuracy of the quantitative results is the standard deviation (STD) determined through triple measurements of QXRD. Whilst quartz, sheet silicates, and other gangue minerals were determined with a STD of less than 5 % (in most cases below 1 %) a larger error was recognized in the analysis of copper sulphides and carbonate minerals of about 12 % on average (Tab. 4, Fig. 3). The high STD reflects difficulties in Rietveld refinement of minerals characterized by a high number of peaks (e.g. chalcocite series), numerous peak overlaps, and some effects of potentially not perfectly random oriented powder samples.

Nonetheless, the results of the Rietveld refinement are marked by a high degree of accordance. An example of the quality of the Rietveld refinement is given in figure 7, especially visible in the difference of fit displayed at the bottom of the diagrams. The observed R-weighted profile R_{wp} ranged from 5 to 10%, indicating a fairly good agreement between observed and calculated diffraction pattern. R_{wp} should approach the R-expected (R_{exp}) error that lies between 3 and 8 %. The calculated goodness of fit (x^2) ranged from 1.3 to 2.3. A minor offset is observed in the fit of the quartz peaks, which reflect larger crystallite sizes due to resistance during milling (Fig. 7).

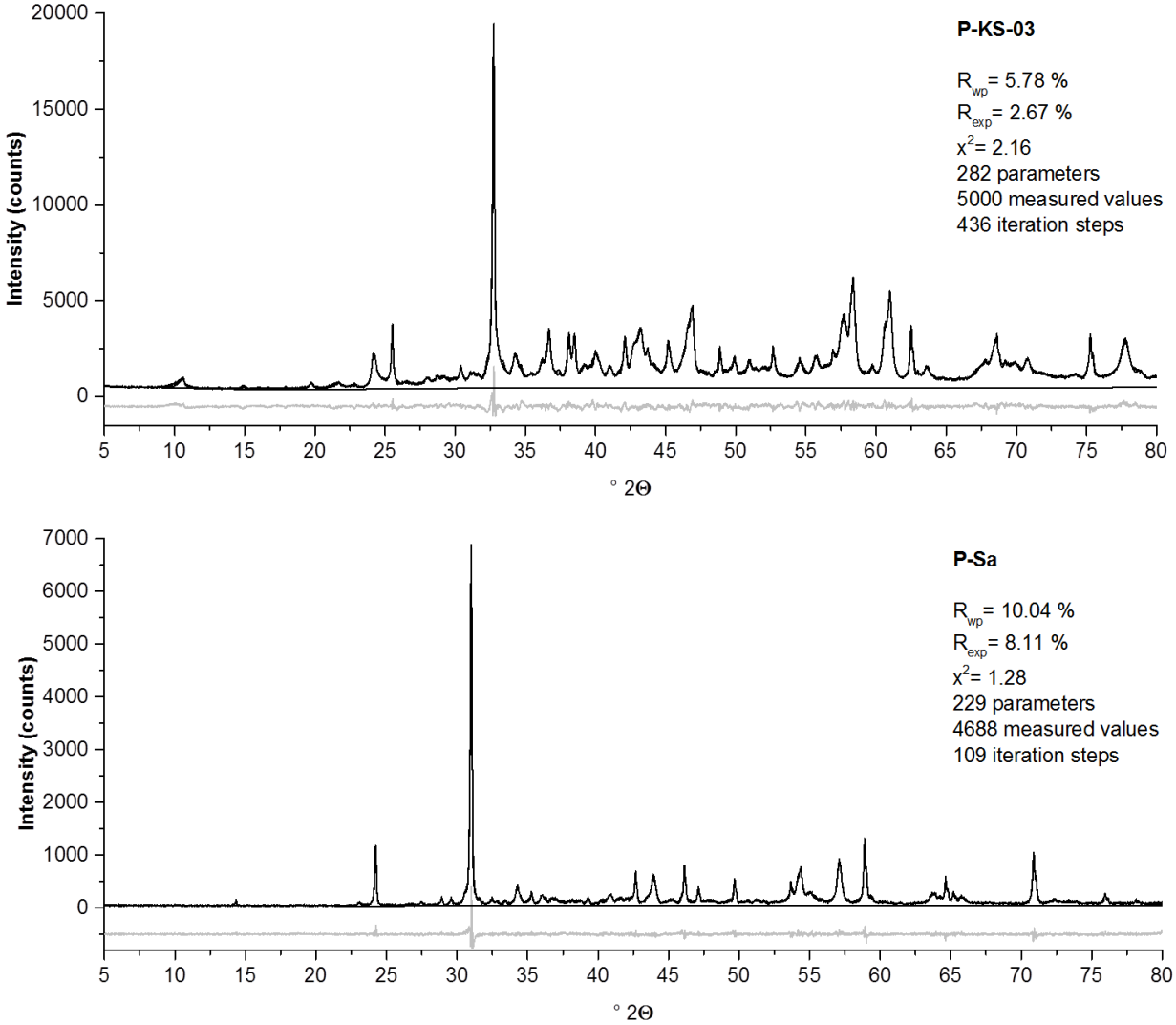

Figure 7: Observed versus calculated XRD pattern with fitted background and difference curve (grey) of Kupferschiefer s.s. (top) and sandstone ore (bottom) from Polkowice-Sieroszowice after Rietveld refinement.

QXRD measurements revealed on average 16 % amorphous content (Fig. 3), which includes organic matter, X-ray amorphous minerals, surface-absorbed water, and unidentified minerals that are not accessible for the quantification by XRD.

3.3 Results of MLA

Clearly distinguishable EDX spectra were collected for each mineral contained within the Kupferschiefer samples, so far as a sufficient chemical difference was observed. No attempt was made to distinguish minerals with a very similar chemistry. This relates in particular to digenite (Cu_9S_5), djurleite ($Cu_{31}S_{16}$), and roxbyite ($Cu_{1.78}S$), that were all grouped together as chalcocite. Although an individual distinction between chlorite, kaolinite, and white mica was possible, in praxis, the identification and differentiation of sheet silicates was difficult and only partially successful. Kaolinite in particular was commonly not recognized correctly and classified as white mica, since the EDX spectra were often influenced by closely intergrown mica.

The detection of accessory minerals, such as apatite, rutile, and tennantite was completed with high precision, especially in contrast to QXRD. Of special interest was at this the detection of stromeyerite (AgCuS) and Ag-rich varieties of chalcocite, which can provide invaluable information on the association and distribution of Ag within the sample materials. Also, dolomite was distinguished from ankerite with great confidence. Data points carrying signals of multiple minerals with “mixed spectra”, classified as unknowns, amount to an average of below 10%. This is a high percentage of unknowns compared to measurements of less complex

materials with a common content of less than 0.5 %. It largely results of the significantly lower grain sizes associated with Kupferschiefer ores and subsequent generation of mixed spectra along the innumerable grain boundaries, particularly within the matrix.

4. Discussion

To assess the accuracy of QXRD and MLA, especially with regard to the differences observed in copper mineral and sheet silicate concentration and in the absence of any suitable reference standard for Kupferschiefer ores, a comparison with geochemical data was made. Element concentrations were calculated based on respective concentrations of Si, Al, Ca, and Cu contained in all minerals identified (Tab. 3) and their abundance in respective samples. These calculated element abundances were compared to assay data from ICP-OES (Fig. 8). The total organic carbon was included in the calculation and the data corrected. An in-depth investigation into the accuracy of chemical assay data for Kupferschiefer (Rahfeld et al., submitted 2017) yielded analytical errors of 5 (Cu) to 12 % (Al). These errors are taken into consideration.

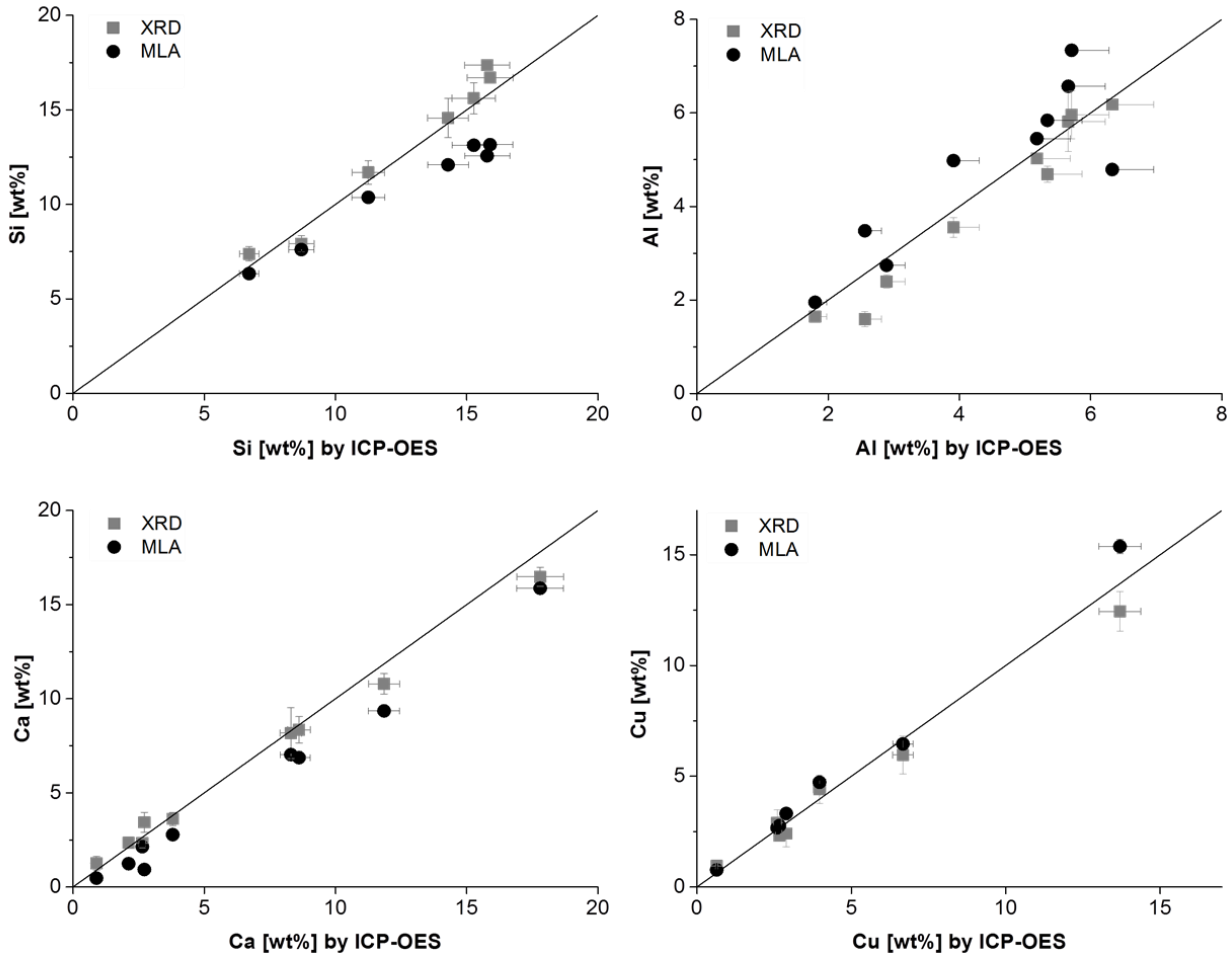

Figure 8: Concentrations of Si, Al, Ca, and Cu calculated from mineralogical data obtained by QXRD and MLA compared to chemical assays. Error bars represent STD of QXRD and MLA measurements and the relative deviation of ICP-OES data to INAA

The majority of the assay data calculated from MLA and QXRD results are within an error range of 5 to 10 % relative to assay data measured by ICP-OES. This is considered a reasonable result given the uncertainty associated with the geochemical data and complexity of the material. An interesting discrepancy is observed between MLA and QXRD data when considering Si and Al concentrations. Si contents, reflecting the abundance of quartz, feldspars, and sheet silicates, as calculated from QXRD, deviate on average only 6% from the measured assay data. Concentrations of Al values calculated from QXRD, in contrast, are consistently below those

obtained by ICP-OES, by an average of about 12 % (Fig. 8), and indicate an underestimation of the sheet silicate content. The exact opposite is observed for assays calculated from MLA data, where Si is systematically below and Al in all but one case above the chemical assay. It appears thus that small, systematic, and largely complementary errors mark the QXRD and MLA data sets with regards to sheet silicate and quartz abundances.

In contrast, deviations of calculated assays for the concentration of Ca from the measured chemical assay are rather similar for QXRD and MLA. In both cases, a usually minor but nevertheless systematic underestimation is apparent (Fig. 8). Good is the agreement for Cu concentrations for all three data sets (ICP-OES, MLA, QXRD; Fig. 8) with average deviations around 10% or less. Obvious deviations are limited to the Cu flotation concentrate sample.

Comparison of quantitative mineralogical and chemical data illustrate that both MLA and QXRD possess inherent strengths and weaknesses that influence the results and explain the underlying reason for the observed systematic trends towards either under- or overestimation (Tab. 5). While the table and discussion place a large focus on inherent weaknesses that are brought out by this challenging raw material, the strengths of the methods cannot be understated. QXRD was able to supply highly representative bulk analytical results and could, when processed carefully, reveal mineralogical characteristics in great detail such as varieties in the present copper sulphides and sheet silicates. Similarly robust quantitative mineralogical data was obtained by MLA for major minerals. A unique strength of MLA is the detection and quantification of trace mineral abundancies and changes in chemical mineral composition. The identification of stromeyerite (AgCuS) and Ag-rich varieties of chalcocite is of particular importance in the case of Kupferschiefer ores, due to the economic significance of Ag for Kupferschiefer mining and beneficiation procedures. Calculation of the Ag assay from

stromeyerite and Ag-rich chalcocite abundancies (in samples W-KS, R-KS, P-KS-2, P-KS-3, and L-KS-Con) yield contents of 100-1000 ppm, a range that is elevated but typical for the studied Kupferschiefer ores.

Table 5: Technique-specific sources of error in MLA and QXRD

	QXRD	MLA
Preparation	• preferred orientation • amorphisation of during micronization	• sedimentation effects/ influence of grain shapes • loss of minerals in preparation of grain mounts
Measurement	• no detection of amorphous material	• no detection of organic matter • difficulties with small grains (<5 µm) • insufficient excitation at 15 kV of heavier elements (e.g. Cu)
Processing	• peak overlaps (decreased precision, high STD) • misidentification (similar crystallography)	• Unknowns (mixed spectra) create bias(commonly of fine-grained carbonates and sheet silicate dominated matrix)
Representativity	*bulk material analysis*	*limited to 2D surfaces, influenced by particle shape and size*

4.1. Specific analytical challenges of MLA

Under the conditions presented in this study, MLA could deliver highly detailed and robust quantitative mineralogical information, especially of minerals in low concentrations. Different to QXRD, MLA data also provide constraints on important textural attributes, including grain size, association and liberation. Nevertheless, MLA data obtained for the Kupferschiefer are marked by systematic overestimation of the sheet silicate abundance, as suggested by high Al concentrations in the calculated assays (Fig. 8). This can be attributed to the difficulty to accurately identify sheet silicates that are finely intergrown and have grain sizes well below 5

µm (Schofield et al., 2002). To counter this effect in this study, an acceleration voltage of only 15 kV was used. This reduced the abundance of disturbed spectra, also referred to as unknowns, by minimizing the size of the excitation volume. As a result, and in comparison to data obtained at 25 kV acceleration voltage, the amount of unknowns was greatly reduced, abundance of detected sheet silicates increased, and the abundance of copper sulphides decreased to a reasonable amount. The use of 15 kV acceleration voltage did, however, yield to a bias towards sheet silicates. A likely reason for the overestimation of the sheet silicate content is suspected to lie in the foremost platy and flat mineral shape of sheet silicates in contrast to more isometric sulphide minerals. Spectra from the edges of sheet silicates occasionally show a strong signal of the epoxy – an indication of its thinness. The 2D-nature of the MLA method make it dependent on particle shapes, sizes, and density, all of which might affect the quantified phase abundance (Kwitko-Ribeiro, 2011; Heinig et al., 2015). Depending on the view, or rather cut of the sample, a greater surface area of platy sheet silicates is visible horizontally than in comparison to a perpendicular cut. The precise effect of sample preparation and the influence of mineral properties should therefore be investigated in future studies. A future approach incorporating a diagonally cut grain mount surface might reduce potential stratification and the effect of mineral orientation and shape (Kwitko-Ribeiro, 2011) . It could however, also have an adverse effect on the quantification of platy sheet silicates, due to a further decrease of the already small mineral surface area and decrease the signal quality.

In addition, it appears likely that a large fraction of the unknowns is composed of carbonate minerals, often occurring in the interstices of the Kupferschiefer matrix, explaining the observed underestimation of the carbonates recognized by low calculated Ca concentrations (Fig. 8) and causing a corresponding increase in sheet silicate abundances. A further factor influencing the

quantitative results of MLA could be the loss of soluble or soft minerals, gypsum in particular, in the course of sample preparation. This effect is less noticeable in primary Kupferschiefer ores that contain 0.3 – 3 wt% gypsum. To minimize this problem, water-free preparation should be considered.

An accurate assessment of particle sizes and liberation might be also inhibited by an abundance of C_{org}. Solid organic material (C_{org}) present in the the Kupferschiefer s.s. (Fig. 1) cannot readily be differentiated from the epoxy resin in which the process samples are typically embedded. This problem can be circumvented by using alternate embedding media, like iodized epoxy resin (Rahfeld and Gutzmer, 2017).

4.2. Specific analytical challenges of QXRD

QXRD is an invaluable tool for mineralogical analysis and provided comprehensive quantitative results on the mineralogical composition of Kupferschiefer ores with good accuracy. QXRD appears to deliver the most accurate results for silicates and could further differentiate members of the chalcocite-series, which can be valuable in monitoring processing effects. However, a number of factors can affect the accuracy of the Rietveld refinement. These have to be considered and evaluated to fully reap the benefits QXRD can deliver.

In the case of Kupferschiefer ores, a minor but nevertheless systematic underestimation of the Cu content in the calculated assays is apparent. This relates to a corresponding underestimation of Cu sulphide abundances. Potential insufficient correction of micro-absorption effects, resulting from the contrast of X-ray absorption between minerals (Bish and Reynolds, 1989; linear absorption coefficients (Co-Kα): Qz 146 cm^{-1}, Ms: 163 cm^{-1}, Bn: 467 cm^{-1}, Cct: 522 cm^{-1}), could not explain the observed deviation. Laser granulometric measurements of the samples L-

KS-Con, P-KS-2, R-Sa showed no increased grain sizes, D_{50} ranging from 3.3 to 4.7 µm, refuting the strongly crystallite size-dependent absorption effects as source of this error. Also, the absorption contrast between the silicates and copper minerals is much weaker than those of synthetic mixtures that could be successfully quantified with Brindley corrections by Taylor and Matulis (1991) . Therefore, we come to the conclusion that the Brindley correction (Brindley, 1945) of the micro-absorption used in the BGMN software, the application of Co radiation, and the micronization of the sample material could successfully counter any absorption effects. Considering the goodness of fit achieved with the Rietveld refinement, another source of error was investigated. Sample preparation designed to minimize micro-absorption and crystallite size effects by micronizing material in a ball mill appears to induce a bias into the analyses. Test measurements of simple synthetic mixtures composed of quartz, illite, muscovite, ankerite, bornite and chalcocite; have indicated a similar overestimation of quartz and underestimation of bornite and chalcocite by QXRD. A further investigation of pure quartz, bornite and chalcocite, after passing the micronization mill with the addition of an internal standard, showed a strongly increased amorphous content in the copper sulphides of about 25 wt % compared to 6 % within quartz. This might not necessarily be related to amorphization but also line broadening and a not ideal fit of the much more complex copper sulphide structures. This study therefore concludes that a fraction of comparatively soft copper sulphides are either potentially damaged in the sample preparation procedure or not appropriately described and therefore underestimated to a stronger degree.

In addition, quantification of copper minerals was accompanied by high STD, caused by the low abundance of the single minerals commonly ranging below 2 wt%. In contrast to MLA, XRD distinguished between more types of copper sulphides based on their differing crystal

structures. The overall amount of each phase is therefore further decreased, but accompanied by more peaks at close range and an increase of peak overlaps. QXRD is not applicable to accurately determine such low mineral abundances within Kupferschiefer ores. The d-space range of 0.1 to 0.3 nm is covered in most analyses of Kupferschiefer s.s. almost entirely by peaks. Although Rietveld refinement is able to handle a certain degree of peak overlaps (Will, 2006), this can be too much and is reflected in a high STD, in particular of minor accessory minerals, and make a correct calculation less probable.

A major issue for quantitative XRD analyses is the perfectly random orientation of the sample for the measurement. Relative intensities of minerals settling in preferred orientations will be distributed unevenly and affect the quantification (Bish and Reynolds, 1989; Moore and Reynolds, 1989), in addition to any grain size effects . This is of particular interest in the presence of large amounts of sheet silicates as, for example, found in Kupferschiefer s.s. An alternate technique to guarantee optimal measurement condition is preparation of the sample by spray-drying (Hillier, 1999; Kleeberg et al., 2008). Small scale tests of spray-drying were undertaken on a subset of the samples (L-KS-Con, P-KS-3, M-KS). The QXRD measurements of the spray-dried samples showed no differences to the ones prepared by side-loading (all results within the STD of the side-loaded samples), implying that preferred orientation is unlikely to have affected the quantification of the sheet silicates to a significant degree. Overall, quantification of the sheet silicates is satisfactory. The observed underestimation is most likely caused by the insufficient structure models for white mica and mica-smectite interstratifications. As the used ideal structure models did not allow the description of the extremely broadened peaks of the disordered varieties, it can be assumed that the

underestimation of the sheet silicates (and the overestimation of the amorphous content) could be reduced by the development of adequate models taking into account the real disorder, or, alternatively, by the application of calibrated *hkl* files (Taylor and Matulis, 1994).

5. Conclusion

QXRD and MLA are able to quantitatively assess the mineralogical composition of Kupferschiefer ores successfully with a relative deviation of ±10 % for both main and trace elements, despite the intricacies inherent to Kupferschiefer ores. A flawless quantitative determination of the mineralogy in Kupferschiefer-type ores appears to be impossible by a single analytical method, considering the difficulties imposed by the material itself and physical constraints of the techniques used. It is essential to follow an iterative path of repeated cross-verification between different methods (in this case QXRD, MLA, and chemical assay data). Assuming proper verification and correction, robust and accurate results can be achieved for all relevant mineral groups.

The combination of MLA and QXRD measurements demonstrate a suitable to approach for routine analysis and give a holistic view into Kupferschiefer ore compositions. The presented strategy also has potential for bulk mineralogical studies of other complex materials that are derived from primary sources or beneficiation processes and are characterized by fine grain sizes or a complex mineralogical composition.

Acknowledgements:

We are grateful to Andreas Kamradt and Raik Döbelt of the Martin-Luther-University Halle-Wittenberg for supplying the black shale sample from the underground Wettelrode Fortschritt

shaft. The authors would also like to thank KGHM Polska Miedź S.A. and KGHM Cuprum who provided access to the mines and supplied samples of the copper concentrate. Laser granulometry measurements were provided by Klaus Meier from the Helmholtz-Institute Freiberg. This work was part of the EcoMetals project and was financially supported by the German Ministry of Education and Research BMBF (Ref. Nr. 033RF001).

Tables

Table 1: List of sampling locations and lithological types (* an industrial sulphide flotation concentrate originating from a mixture of Kupferschiefer black shale, sandstone, and carbonate)

Table 2: ICP-OES data used in the data validation *(values in wt%)*

Table 3: List of identified and Rietveld refined minerals considered for Rietveld refinement – and the grouping applied to the data for comparability (sorted based on relative abundance)

Table 4: List of quantitative mineralogical results in wt %

Table 5: Technique-specific sources of error in MLA and QXRD

Figures

Figure 1: A- Photomicrograph of Kupferschiefer s.s. sample P-KS-02 (left) illustrating the fine-grained texture of the sheet silicate and carbonate-rich matrix (M) with irregular lenses and layers of organic matter (Corg). B- Photomicrograph in reflected light of sample P-KS-03 showing dissemination of copper sulphides (S, black arrows)

Figure 2: Schema of method-specific characteristics and advantages

Figure 3: Illustration of quantitative mineralogical results of QXRD (X) and MLA at 15 (15) and 25 kV (25). Results normalized to 100 wt% excluding unknowns and amorphous contents.

Figure 4: XRD patterns of oriented aggregates after heat treatment (left), used to identify proportions of kaolinite (Kln) and dickite (Dck), and glycolation with ethylene glycol (right), used to identify fractions of illite-smectites (I/S)

Figure 5: Selection of oriented XRD measurements (left) illustrating the variety of clay minerals associated with Kupferschiefer ores and patterns of randomly oriented samples (right) prepared by spray-drying showing white mica polytpes based on Drits et al., 1993 (d-values in Å, Chl:

chlorite, I/S: mica-smectite, M: white mica, Q: quartz, Kln: kaolinite, Dck: dickite, Dol: dolomite, A: atacamite, Ccp: chalcopyrite)

Figure 6: Portion of diffractogram illustrating the change in the copper sulphide mineralogy of sample P-KS-3 within a fresh (top) and an aged, 6-month old sample (bottom)

Figure 7: Observed versus calculated XRD pattern with fitted background and difference curve (grey) of Kupferschiefer s.s. (top) and sandstone ore (bottom) from Polkowice-Sieroszowice after Rietveld refinement

Figure 8: Concentrations of Si, Al, Ca, and Cu calculated from mineralogical data obtained by QXRD and MLA compared to chemical assays. Error bars represent STD of QXRD and MLA measurements and the relative deviation of ICP-OES data to INAA

References

Arslan, C. and Arslan, F. (2002) 'Recovery of copper, cobalt, and zinc from copper smelter and converter slags', *Hydrometallurgy,* No. 67, pp.1–7.

Bailey, S.W. (1984) 'Classification and structures of the micas', *Mineralogical Society of America, Reviews in Mineralogy,* No. 13.

Bailey, S.W. (1963) 'Polymorphism of kaolin minerals', *American Mineralogist,* No. 48, pp.1196–1209.

Bechtel, A., Elliott, W.C., Wampler, J.M. and Oszczepalski, S. (1999) 'Clay Mineralogy, Crystallinity, and K-Ar Ages of Illites within the Polish Zechstein Basin: Implications for the Age of Kupferschiefer Mineralization', *Economic Geology,* No. 94.

Bechtel, A., Shieh, Y.-N., Elliott, W.C., Oszczepalski, S. and Hoernes, S. (2000) 'Mineralogy, crystallinity and stable isotopic composition of illitic clays within the Polish Zechstein basin: implications for the genesis of Kupferschiefer mineralization', *Chemical Geology,* No. 163.

Bergmann, J. and Kleeberg, R. (1998) 'Rietveld analysis of disordered layer silicates', *Materials Science Forum,* 278-281, pp.300–305.

Bioshale Project (2007) 'Publishable Activity report'.

Birle, J.D. and Tettenhorst, R. (1968) 'Refined Muscovite structure', *Mineralogical Magazine,* No. 36.

Bish, D.L. (1993) 'Rietveld refinement of the kaolinite structure at 1.5 K', *Clays and Clay Minerals,* No. 41, pp.738–744.

Bish, D.L. (1988) 'Quantitative phase analysis using the Rietveld method', *Applied Crystallography,* No. 21, pp.86–91.

Bish, D.L. and Reynolds, R.C. (1989) 'Sample Preparation for X-ray', in Bish, D.L. and Post, J.E. (Eds.), *Modern Powder Diffraction*, American Reviews in Mineralogy, pp.73–99.

Borg, G., Piestrzynski, A., Bachmann, G.H., Püttmann, W., Walther, S. and Fiedler, M. (2012) 'An Overview of the European Kupferschiefer Deposits', *Economic Geology Special Publication,* No. 16, pp.455–486.

Brindley, W. (1945) 'The effect of grain or particle size on X-ray reflections from mixed powders and alloys, considered in relation to the quantitative determination of crystalline substances by X-ray methods', *Philosophical Magazine and Journal of Science,* No. 36, pp.347–359.

Doebelin, N. and Kleeberg, R. (2015) 'Profex: a graphical user interface for the Rietveld refinement program BGMN', *Applied Crystallography,* No. 48, ?

Drits, V.A., McCarty, D.K., Sakharov, B. and Milliken, K.L. (2005) 'New insight into structural and compositional variability in some ancient excess-Ca dolomite', *The Canadian Mineralogist,* No. 43, pp.1255–1290.

Drits, V.A., Weber, F., Salyn, A.L. and Tsipursky, S.I. (1993) 'X-ray identification of one-layer illite varieties: Application to the study of illites around uranium deposits of Canada', *Clays and Clay Minerals,* No. 41, pp.389–398.

Gu, Y. (2003) 'Automated Scanning Electron Microscope Based Mineral Liberation Analysis: An Introduction to JKMRC/FEI Mineral Liberation Analyser', *Minerals and Material Characterization and Engineering,* No. 2.

Heinig, T., Bachmann, K., Tolosana-Delgado, R., Van Den Boogaart, G. and Gutzmer, J. (2015) 'Monitoring gravitational and particle shape settling effects on MLA sampling preparation', *Proceedings of IAMG 2015 - 17th Annual Conference of the International Association for Mathematical Geosciences*, pp.200–206.

Hill, R.D. (1955) '14 Å spacings in kaolin minerals', *Acta Crystallographia,* No. 8.

Hill, R.J. and Howard, C.J. (1987) 'Quantitative phase analysis from neutron powder diffraction data using the Rietveld method', *Applied Crystallography,* No. 20.

Hillier, S. (2000) 'Accurate quantitative analysis of clay and other minerals in sandstones by XRD: comparison of a Rietveld and a reference intensity ratio (RIR) method and the importance of sample preparation', *Clay Minerals,* No. 35.

Hillier, S. (1999) 'Use of an Air Brush to Spray Dry Samples for X-ray Powder Diffraction', *Clay Minerals,* No. 34.

Jackson, M.I. (1979) 'Mineral fractionation for soils', in Jackson, M.L. (Ed.), *Soil Chemical Analysis. Advanced Course*, Madison, Wisconsin USA, pp.100–166.

Kern, M., Möckel, R., Krause, J., Teichmann, J. and Gutzmer, J. (2017) 'Calculating the deportment of a fine-grained and compositionally complex Sn skarn with a modified approach for automated mineralogy', *Process Mineralogy 2017*, Conference Paper.

KGHM Polska Miedź (2015) *Mineral resources and reserves report. as at December 31, 2014*.

Kleeberg, R., Monecke, T. and Hillier, S. (2008) 'Preferred Orientation of Mineral Grains in Sample Mounts for Quantitative XRD Measurements: How Random are Powder Samples?', *Clays and Clay Minerals,* No. 56.

Kodali, P., Dhawan, N., Depci, T., Lin, C.L. and Miller, J.D. (2011) 'Particle damage and exposure analysis in HPGR crushing using selected copper ores for column leaching', *Minerals Engineering,* No. 163, pp.361–384.

König, U. and Spicer, E. (2007) 'X-ray diffraction (XRD) as a fast industrial analysis method for heavy mineral sands in process control and automation - Rietveld refinement and data clustering', *6th International Heavy Minerals Conference 'Back to Basics'*.

Kucha, H. (1993) 'Noble Metals Associated with Organic Matter, Kupferschiefer, Poland', *Geology Applied to Mineral Deposits Special Publication,* No. 9.

Kucha, H. (1982) 'Platinum-group metals in the Zechstein copper deposits, Poland', *Economic Geology,* No. 77.

Kucha, H. and Pryblowicz, W. (1999) 'Noble metals in organic matter and clay-organic matrices, Kupferschiefer, Poland', *Economic Geology,* No. 94.

Kutschke, S., Guézennec, A.G., Hedrich, S., Schippers, A., Borg, G., Kamradt, A., Gouin, J., Giebner, F., Schopf, S., Schlömann, M., Rahfeld, A., Gutzmer, J., D'Hugues, P., Pollmann, K., Dirlich, S. and Bodénan, F. (2015) 'Bioleaching of Kupferschiefer blackshale – A review including perspectives of the Ecometals project', *Minerals Engineering,* No. 75.

Kwitko-Ribeiro, R. (2011) 'New sample preparation developments to minimize mineral segregation in process mineralogy', *10th International Congress for Applied Mineralogy*, pp.411–417.

Large, D.J., MacQuaker, J. and Vaughan, D.J. (1995) 'Evidence for low-temperature alteration of sulfides in the Kupferschiefer copper deposits of southwestern Poland', *Economic Geology,* No. 90.

Lund, C. and Lamberg, P. (2014) 'Geometallurgy - A tool for better resource efficiency', *European Geologist,* No. 37.

Matlakowska, R., Sklodowska, A. and Nejbert, K. (2012) 'Bioweathering of Kupferschiefer black shale (Fore-Sudetic Monocline, SW Poland) by indigenous bacteria: implication for dissolution and precipitation of minerals in deep underground mine', *FEMS Microbiology Ecology,* No. 81.

Michalik, M. and Sawlowicz, Z. (2001) 'Multi-stage and long-term origin of the Kupferschiefer copper deposit in Poland', in Piestrzynski, A. (Ed.), *Mineral Deposits at the Beginning of the 21st Century*, pp.235–238.

Moore, D.M. and Reynolds, R.C. (1989) 'Sample preparation techniques for clay minerals', in , *X-ray Diffraction and the Identification and Analysis of Clay Minerals*, Oxford University Press, New York, pp.179–201.

Omotoso, O., McCarty, D.K., Hillier, S. and Kleeberg, R. (2006) 'Some successful approaches to quantitative mineral analysis as revealed by the 3rd Reynolds Cup contest', *Clays and Clay Minerals,* No. 54.

Parian, M., Lamberg, P., Möckel, R. and Rosenkranz, J. (2015) 'Analysis of mineral grades for geometallurgy: Combined element-to-mineral conversion and quantitative X-ray diffraction', *Minerals Engineering,* No. 82.

Paul, J. (2006) 'The Kupferschiefer: Lithology, stratigraphy, facies and metallogeny of a black-shale', *Zeitschriften der Deutschen Gesellschaft für Geowissenschaften,* No. 157.

Piestrzynski, A. and Pieczonka, J. (2012) 'Low temperature ore minerals associations in the Kupferschiefer type deposit, Lubin-Sieroszowice Mining District, SW Poland', *Mineralogical Review,* No. 62, pp.59–66.

Piestrzynski, A. and Sawlowicz, Z. (1999) 'Exploration for Au and PGE in the Polish Zechstein copper deposits (Kupferschiefer)', *Geochemical Exploration,* No. 66.

Püttmann, W., Fermont, W.J. and Speczik, S. (1991) 'The possible role of organic matter in transport and accumulation of metals exemplified at the Permian Kupferschiefer formation', *Ore Geology Reviews,* No. 6.

Rahfeld, A. and Gutzmer, J. (2017) 'MLA-based detection of organic matter with iodized epoxy resin – An alternative to carnauba', *Minerals and Materials Characterization and Engineering*, submitted.

Rahfeld, A., Wiehl, N., Möckel, R. and Gutzmer, J. (submitted 2017) 'Major and Trace Element Geochemistry of the European Kupferschiefer – An Evaluation of Analytical Techniques', *Geochemistry: Exploration, Environment, Analysis*.

Rietveld, H. (1967) 'Line profiles of neutron powder-diffraction peaks for structure refinement', *Acta Crystallographia,* No. 22.

Schofield, P.F., Knight, K.S., Covey-Crump, S.J., Cressey, G. and Stretton, I.C. (2002) 'Accurate quantification of the modal mineralogy of rocks when image analysis is difficult', *Mineralogical Magazine*, Vol. 66, No. 1.

Steinfink, H. (1958) 'The crystal structure of chlorite. I. A monoclinic polymorph', *Acta Crystallographia,* No. 11.

Sun, Y. and Püttmann, W. (2004) 'Composition of kerogen in Kupferschiefer from southwest Poland', *Chinese Journal of Geochemistry,* No. 23.

Taylor, J.C. and Matulis, C.E. (1994) 'A new method for Rietveld clay analysis. Part I. Use of a universal measured standard profile for Rietveld quantification of montmorillonites', *Powder Diffraction,* No. 9.

Taylor, J.C. and Matulis, C.E. (1991) 'Absorption contrast effects in the quantitative XRD analysis of powders by full multiphase profile refinement', *Applied Crystallography,* No. 24, pp.14–17.

Tsipursky, S.I. and Drits, V.A. (1984) 'The distribution of octahedral cations in the 2: 1 layers of dioctahedral smectites studied by oblique-texture electron diffraction', *Clay Minerals,* No. 19, pp.177–193.

Ufer, K., Kleeberg, R., Bergmann, J. and Dohrmann, R. (2012) 'Rietveld Refinement Of Disordered Illite-Smectite Mixed-Layer Structures By A Recursive Algorithm. Ii: Powder-Pattern Refinement And Quantitative Phase Analysis', *Clays and Clay Minerals,* No. 60.

Van den Boogart, K.G., Weißflog, C. and Gutzmer, J. (2011) 'The value of adaptive mineral processing based on spatially varying ore fabric parameters', *Proceedings of IAMG, September 5-11, University of Salzburg, Austria*.

Vaughan, D.J., Sweeney, M.A., Friedrich, G., Diedel, R. and Haranczyk, C. (1989) 'The Kupferschiefer; an overview with an appraisal of the different types of mineralization', *Economic Geology,* No. 84.

Vorster, W., Rowson, N.A. and Kingman, S.W. (2001) 'The effect of microwave radiation upon the processing of Neves Corvo copper ore', *International Journal of Mineral Processing,* No. 63, pp.29–44.

Wedepohl, K.H. (1964) 'Untersuchungen am Kupferschiefer in Nordwestdeutschland; Ein Beitrag zur Deutung der Genese bituminöser Sedimente', *Geochimica et Cosmochimica Acta,* No. 28.

Will, G. (2006) *Powder Diffraction. The Rietveld Method and the Two-Stage Method to Determine and Refine Crystal Structures from Powder Diffraction Data,* Springer-Verlag, Berlin Heidelberg.

Zeelmaekers, E., McCarty, D. and Mystkowski, K. (2007) 'SYBILLA user manual', *Chevron proprietary software,* Texas, USA.